



Synthesis, Characterization and *In silico* Molecular Docking Studies of Novel Chromene Derivatives as Rab23 Inhibitors



Awatef M. El-Maghraby and Aboubakr H. Abdelmonsef*

Chemistry Department, Faculty of Science, South Valley University, Qena 83523, Egypt

THE Rab23 protein overexpression has a well-validated role in variety of human cancers. Therefore, the present research aimed to identify new Rab23 protein inhibitor candidates using computational based drug design methodology. A novel series of chromeno[2,3-b] pyridine derivatives has been synthesized by the cyclocondensation of 2-amino-3-cyano-4H-chromenes with cyclohexanone and cyclopentanone in ethanolic piperidine solution. The 2-amino-4H-chromenes were obtained using one pot multicomponent condensation of resorcinol, malononitrile and aromatic aldehydes in the presence in ethanolic piperidine solution. All newly synthetic compounds were characterized by spectral analysis IR, NMR and MS and elemental analysis techniques. The best binding modes of chromene derivatives were evaluated via molecular docking studies and binding energy calculations, using PyRx tool. The study has shown that the pyran and pyridine moieties interact favorably with the binding site of target protein, providing the mechanism of action against human sapiens Rab23 protein.

Keywords: Synthesis, 4H-Chromenes, Rab23 protein, *In silico*, Binding site.

Introduction

Upregulation of Rab23 protein in human beings plays a crucial role in gastric cancer progression through signaling pathway [1]. In the present work, we employed several computational approaches for design of novel Rab23 inhibitors. The chromene derivatives are considered as the key structural compounds for many drugs having a broad spectrum of medicinal and pharmaceutical chemistry, because of their multiplicity uses in drug industry [2], [3]. Additionally, the chromene nucleus is an important pharmacophore in many biologically active compounds [4], [5]. Based on the above mentioned chemistry and biology significance of chromene analogue, a series of promising chromene derivatives **4-6** has been synthesized. In addition, we investigated *In silico* the newly synthetic compounds against Rab23 protein inhibition using molecular docking approach. As the crystal structure of Rab23 is not available in protein data bank, we computationally generated

its (3D) three dimensional structure depending on its closet homolog protein (template). Moreover, the binding site was predicted using different tools. *In silico* molecular docking approach was successfully applied to enlighten the binding affinity and the conformational stability between the newly synthetic chromene derivatives and the cancer target protein. Also, the pharmacophoric and physicochemical properties of the derivatives were investigated. Altogether, our study identifies potential inhibitors of Rab23 protein, for further investigation as gastric anticancer agents.

Experimental

Chemistry

All melting points were measured with a Gallenkamp apparatus. The IR spectra of samples were recorded in KBr via a Shimadzu FT-IR 8101 PC infrared spectro photometer. The NMR spectra were run at 300MHz using TMS as the internal standard. Chemical shifts were measured

*Corresponding author e-mail: aboubakr.ahmed@sci.svu.edu.eg. Tel. 00201098965494.

Received 21/07/2019; Accepted 23/8/2019

DOI: 10.21608/ejchem.2019.15013.1911

©2020 National Information and Documentation Center (NIDOC)

in ppm (δ) related to TMS (0.00 ppm). Mass spectra were measured on a GCMS-QP1000 EX spectrometer at 70 eV. TLC was conducted on 0.25 mm precoated silica gel plates (60F-254). Elemental analyses were carried out at the Micro analytical center at Cairo university, Egypt.

General Procedure for the Synthesis of 2-amino-7-hydroxy-4-aryl-4H-chromene-3-carbonitrile (4a-c):

Equimolar amounts of resorcinol, malononitrile and different aromatic aldehydes with piperidine (3 drops) were mixed. The reaction mixtures were heated in refluxing ethanol for 4-6 hrs respectively. After cooling the corresponding, the solid products separated out were collected by filtration and recrystallized from ethanol to give chromenes (**4a-c**).

2-amino-4-(4-(benzyloxy)phenyl)-7-hydroxy-4H-chromene-3-carbonitrile(4a) m.p.250 °C yield 92 %. IR (KBr, cm^{-1}):3343, 3206,2924,2855, 2362, 2190, 1655, 1624, 1582,1506.¹H-NMR (300MHz, DMSO): 4.55 (s, 1H, H-4), 5.05 (s,2H,-CH₂-), 6.38 (s, 2H, NH₂), 6.39-6.46 (m, 3H, Ar-H), 6.48 - 6.92 (m,4H,Ar-H), 7.33-7.45 (m, 5H, Ar-H), 7.06 (s, 1H, OH). M.S (m/z): 370.13 (34.7%), 371.14 (8.77%), 372.14 (1.34%). Anal. calcd for C₂₃H₁₈N₂O₃: C,74.58; H,4.90;N,7.56.Found: C,74.45; H,4.85;N,7.49.

2-amino-4-(2,6-dichlorophenyl)-7-hydroxy-4H-chromene-3-carbonitrile (4b) m.p. 275 °C yield 90 %. IR (KBr, cm^{-1}) 3539, 3334, 3207, 2938, 2187, 1657, 1559, 1508. ¹H-NMR (300 MHz, DMSO): 5.69 (s, 1H, H-4), 6.90 (s, 2H, NH₂), 6.36-6.44 (m, 3H, Ar-H), 6.35 (s, 1H, OH), 7.29-7.33 (m, 3H, Ar-H). M.S (m/z): 332.95 (5.03%), 333.95 (6.77%), 334.95 (1.8%). Anal. calcd for C₁₆H₁₀N₂O₂Cl₂: C, 57.68; H, 3.03; Cl, 21.28; N, 8.41. Found: C, 57.65; H, 2.95; Cl, 21.20; N, 8.32.

2-amino-4-(2,3dimethoxyphenyl)-7-hydroxy-4H-chromene-3-carbonitrile (4c) m.p. 251 °C yield 85%. IR (KBr, cm^{-1}) 3419, 3327, 2937, 2838, 2190, 1661, 1508. ¹H-NMR (300 MHz, DMSO): 3.65 (s, 3H, OCH₃), 3.70 (s, 3H, OCH₃), 4.89 (s, 1H, H-4), 6.75 (s, 2H, NH₂), 6.45-6.74 (m, 6H, Ar-H), 9.61 (br s, 1H, OH). Anal. calcd for C₁₈H₁₆N₂O₄: C,66.66; H,4.97; N, 8.64. Found: C, 66.41; H, 5.12; N, 8.54 [6].

General procedure for the synthesis of 11-amino-12-(aryl)-8,9,10,12-tetrahydro-7H-chromeno[2,3-b]quinolin-3-ol (5a-c)

A mixture of cyclohexanone (1 mmol) with chromenes (**4a-c**) (1 mmol) in 15 mL ethanol in the presence of piperidine was refluxed for 6:9 hrs respectively. The solid products, so formed, were filtered off and recrystallized to afford (**5a-c**).

11-Amino-12-(4-(benzyloxy)phenyl)-8,9,10,12-tetrahydro-7H-chromeno[2,3-b]quinolin-3-ol (5a) m.p. 260 °C yield 72 %. IR (KBr, cm^{-1}): 3334, 3227, 2944, 2835. ¹H-NMR (300 MHz DMSO): 1.76 (m, 4H, 2CH₂), 2.73 (m,2H,CH₂), 3.02 (m,2H,CH₂), 5.31(s, 1H, CH), 5.14(s,2H,-CH₂O), 6.23(s, 2H, NH₂), 6.14-7.11 (m,7H,Ar-H), 7.33-7.44 (m, 5H, Ar-H), 5.33 (s, 1H, OH). ¹³CNMR: δ 22.4, 26.6, 30.1, 33.3, 70.0, 87.0, 98.1, 109.4, 112.6, 113.9, 115.1, 115.3, 127.7, 127.9, 128.2, 128.3, 128.5, 128.9, 129.1, 129.2, 129.3, 136.3, 136.7, 146.4, 155.8, 160.4, 160.9, 161.4, 161.9. M.S (m/z): 450.19 (100.0%), 451.20 (31.7%), 452.21 (5.6%). Anal. calcd for C₂₉H₂₆N₂O₃: C, 77.31; H, 5.82; N, 6.22. Found: C, 77.81; H, 5.32; N, 6.34.

11-amino-12-(2,6-dichlorophenyl)-8,9,10,12-tetrahydro-7H-chromeno[2,3-b]quinolin-3-ol(5b) m.p. 245° C yield 75 %. IR (KBr, cm^{-1}): 3540, 3335, 3204, 2924, 2854. ¹H-NMR (300MHz, DMSO): 1.47 (m,4H,2CH₂), 2.69 (m,2H,CH₂), 3.44 (m,2H,CH₂) 5.69 (s, 1H, CH), 6.37(s, 2H, NH₂), 7.30-7.55 (m,6H,Ar-H), 6.47 (s, 1H, OH). M.S (m/z): 412.07 (100.0%), 414.07 (64.1%), 413.08 (24.2%), 415.07 (15.8%), 416.07 (10.4%). Anal. calcd for C₂₂H₁₈Cl₂N₂O₂: C, 63.93; H, 4.39; Cl, 17.16; N, 6.78. Found: C, 63.43; H, 4.29; Cl, 17.26; N, 6.73.

11-amino-12-(2,3-dimethoxyphenyl)-8,9,10,12-tetrahydro-7H-chromeno[2,3-b]quinolin-3-ol(5c) m.p. 236° C yield 71%. IR (KBr, cm^{-1}): 3381, 2935,2855. ¹H-NMR (300MHz, DMSO): 1.82 (m, 2H, CH₂), 2.95(m, 4H, 2CH₂), 3.40 (m, 2H, CH₂), 3.87 (s, 3H, OCH₃), 3.76 (s, 3H, OCH₃), 5.03 (s, 1H, CH), 6.72 (s, 2H, NH₂), 6.73-6.87 (m, 6H, Ar-H), 4.06 (s, 1H, OH). M.S (m/z):404.17 (100.0%), 405.18 (26.3%), 406.18 (4.1%). Anal. calcd for C₂₄H₂₄N₂O₄: C, 71.27; H, 5.98; N, 6.93. Found: C, 71.22; H, 5.68; N, 6.63.

General procedure for the synthesis of 11-amino-10-(4-(aryl)-1,2,3,10-tetrahydrochromeno[2,3-b]cyclopenta[e]pyridin-7-ol(6a-c)

A mixture of cyclopentanone (1 mmol) with chromenes (**4a-c**) (1 mmol) in 15 mL ethanol in the presence of piperidine was refluxed for 7hr. The solid product, so formed after cooling, was filtered off and recrystallized from ethanol to give

(6a-c).

11-amino-10-(4-(benzyloxy)phenyl)-1,2,3,10-tetrahydrochromeno[2,3-b]cyclopenta[e]pyridin-7-ol(6a) m.p. 260 °C yield 72 %. IR (KBr, cm^{-1}): 3409, 3226, 2922, 2825. $^1\text{H-NMR}$ (300 MHz, DMSO): 1.84 (m, 2H, CH_2), 3.35 (m, 4H, 2CH_2), 4.78 (s, 1H, CH), 5.16 (s, 2H, $-\text{CH}_2\text{O}$), 6.28 (s, 2H, NH_2), 6.28-6.97 (m, 7H, Ar-H), 7.22-7.51 (m, 5H, Ar-H), 9.19 (s, 1H, OH). M.S (m/z): 436.18 (100.0%), 437.18 (31.3%), 438.19 (4.6%). Anal. calcd for $\text{C}_{28}\text{H}_{24}\text{N}_2\text{O}_3$: C, 77.04; H, 5.54; N, 6.42. Found: C, 77.14; H, 5.34; N, 6.32.

11-amino-10-(2,6-dichlorophenyl)-1,2,3,10-tetrahydrochromeno[2,3-b]cyclopenta[e]pyridin-7-ol (6b) m.p. 245 °C yield 75 %, IR (KBr, cm^{-1}): 3407, 3332, 2922, 2857. $^1\text{H-NMR}$ (300MHz DMSO): 2.24 (m, 2H, CH_2), 3.34 (s, 4H, 2CH_2), 5.69 (s, 1H, CH), 6.37 (s, 2H, NH_2), 6.38-7.57 (m, 6H, Ar-H), 9.76 (s, 1H, OH). M.S (m/z): 398.06 (100.0%), 400.06 (64.6%), 399.06 (23.6%), 401.06 (14.7%), 402.05 (10.2%), 400.07 (2.5%), Anal. calcd for: $\text{C}_{21}\text{H}_{16}\text{Cl}_2\text{N}_2\text{O}_2$: C, 63.17; H, 4.04; Cl, 17.76; N, 7.02. Found: C, 63.27; H, 4.14; Cl, 17.66; N, 7.12.

11-amino-10-(2,3-dimethoxyphenyl)-1,2,3,10-tetrahydrochromeno[2,3-b]cyclopenta[e]pyridin-7-ol(6c) m.p. 215 °C yield 82%. IR (KBr, cm^{-1}): 3410, 2938, 2853. $^1\text{H-NMR}$ (300MHz, DMSO): 1.66 (m, 2H, CH_2), 3.51 (m, 4H, 2CH_2), 3.40 (m, 2H, CH_2), 3.87 (s, 3H, OCH_3), 3.79 (s, 3H, OCH_3), 5.19 (s, 1H, CH), 6.27 (s, 2H, NH_2), 6.56-6.96 (m, 6H, Ar-H), 5.29 (s, 1H, OH). $^{13}\text{CNMR}$: δ 27.7, 30.1, 30.8, 56.2, 61.0, 87.0, 98.1, 112.6, 113.0, 113.9, 116.8, 126.5, 128.2, 128.8, 129.2, 129.4, 144.0, 146.4, 151.2, 153.8, 155.8, 160.9, 161.9. M.S (m/z): 390.16 (100.0%), 391.16 (25.4%), 392.16 (4.0%). Anal. calcd for $\text{C}_{23}\text{H}_{22}\text{N}_2\text{O}_4$: C, 70.75; H, 5.68; N, 7.17. Found: C, 70.35; H, 5.38; N, 7.07.

In silico molecular docking analysis

Herein, *In silico* molecular docking studies are performed using PyRx bioinformatic docking tool [7] to select the best compounds of drug likeness characters. The Schrodinger Maestro software (Maestro, Schrödinger, LLC, New York, NY, 2019) is used to generate the images of (2D) two dimensional structures of docking between compounds and receptor. In addition, the images of 3D structures are generated by discovery studio® visualizer 3.5 (Accelrys Software Inc., San Diego, CA, USA). A 3D model of the target

is constructed using protein structure modeling program: Modeller 9.11 [8]. To evaluate the constructed model, various computational tools like ProSA [9] and ERRAT [10] servers are used. Protein structure analysis (ProSA) is used to evaluate the quality of 3D model. ERRAT program describes the overall quality factor of a protein. The acceptable range is above 50%. The functional site of the target is predicted based on bioinformatics prediction tools like MetaPocket [11] and ProBiS [12] tools. Twelve synthetic chromene compounds are used to generate in-house library dataset based on anticancer activity reported previously [2]. In this paper we performed virtual screening of compounds from database for identifying novel therapeutics for treatment of gastric cancer. *In silico* pharmacokinetic and molecular properties of chromene derivatives are predicted using various software's such as admetSAR [13] and Mol inspiration web based tools (<https://www.molinspiration.com/>) to select the compounds having optimum drug-likeness. The compound with low molecular weight is easily to be transported, diffused and absorbed. Partition coefficient is useful in estimating the distribution of the compound within the body. Topological polar surface area (TPSA) is a good descriptor of drug absorption. While, numbers of H-bonds donors and acceptors are good predictors of oral bioavailability. The number of rotatable bonds is a good descriptor of oral bioavailability of drugs. The best values for the compound with good membrane permeability are $M.wt \leq 500$ g/mol, $\log P \leq 5$, $TPSA \leq 140 \text{ \AA}^2$, number of H-bond acceptors ≤ 10 , number of H-bond donors ≤ 5 , and number of rotatable bonds ≤ 10 . However, these values used as a filter for drug-like properties. The compounds with the acceptable ADMET properties in the permissible range are considered as novel molecules.

Results and Discussion

Chemistry

The aim of the current work is to synthesize 4H-chromene derivatives and to investigate their modes of interactions with Rab23 binding site. The strategy for synthesis of compounds was performed according to the reaction outlined in Scheme 1. Firstly, 2-amino-3-cyano-7-hydroxy-4-aryl-4H-chromenes (4a-c) were obtained using one pot multicomponent condensation of aromatic aldehydes (1), malononitrile (2) and resorcinol (3) in the presence in ethanolic piperidine

solution (Scheme1). The spectroscopic data are in good agreement with the proposed structures of 4H-chromenes (4a-c). The IR (KBr) showed the presence of (OH and NH₂) functions at ν_{\max} : 3539–3343 cm⁻¹ (broad band) and at ν_{\max} : 2190–2187 cm⁻¹ due to (CN) function. Furthermore, ¹H-NMR revealed also, 4.55-5.05 ppm (s, 1H, H-4), 9.61-6.35 ppm (s, 1H, OH), 6.38-6.90 (s, 2H, NH₂).

As a precursor to construct more heterocyclic compounds incorporating pyridine moiety, the 2-amino-4H-chromenes (4a-c) exploit as starting materials to react with cyclohexanone and cyclopentanone in ethanolic piperidine solution to afford the corresponding 11-amino-12-(aryl)-8,9,10,12-tetrahydro-7H-chromeno[2,3-b]quinolin-3-ol (5a-c) (tacrine analogues) and 11-amino-10-(4-(aryl)-1,2,3,10-tetrahydrochromeno[2,3-b]cyclopenta[e]pyridin-7-ol (6a-c) respectively via Friedlander synthesis (Schemes 2 and 3). Structures of compounds (5a-c) and (6a-c) were confirmed based on their micro analytical and spectral data.

In silico studies

Rab23 model generation and validation

The amino acid sequence of Rab23 (237 aa) was downloaded from Uniprot database [14]. 2bcg protein of highest similarity with the target, was selected as a template using NCBI BLAST server [15]. A pairwise sequence alignment of both proteins was performed using ClustalW, to ensure the presence of conserved motifs. The alignment was subjected to an automated homology modeling program: Modeller 9.11 for creating 3D model of the target.

The homologue model consists of nine helices and six strands obtaining from PDBsum server [16], as represented in Figures 1 and 2. The physicochemical parameters of Rab23 were computed using ProtParam tool. The molecular weight is 26659 Da and the isoelectric point (pI) is 6.22. The results show that the residues LYS, VAL, GLU, LEU, SER, ALA and ASN represent the high percentage in Rab23.

ProSA server results show a Z-score value of -4.57 for protein structure, as presented in Figure 3. The score is within the range of the PDB proteins evaluated by X-ray and NMR, predicting a good quality model. Furthermore, The ERRAT evaluation method (Figure 4) of homologue

model gave 84.64 % as the overall quality factor, indicating a high quality and therefore considered reliable for further studies.

Binding site prediction, molecular docking simulation

The binding site is specific region of a protein which is responsible for binding with ligand molecules [17-19]. Computational approaches like MetaPocket and ProBiS were used to predict the binding region. The results show that the amino acid residues LYS11, ALA19, LYS22, TRP63, THR65 and ARG80 are involved in the interaction with the ligand molecules. A grid box was then generated around the site region with dimensions 25Å° × 25Å° × 25Å° for docking purpose. The 2D chemical confirmations of the synthesized molecules by our research group were generated in cdx format then were converted to sdf files by using OpenBabel 2.4.1 tool [20], and were further used for docking to protein. Identification of compound-target interactions acts as a key role in drug design [21]. The present study performed *In silico* docking approach to prevent cancer in human beings using chromene compounds. However, the ligand-protein simulations were carried out using PyRx screening tool. Twelve synthetic compounds were subjected to virtual screening approach, which has resulted nine conformers for each ligand-protein complex (Figures 5).

Out of the twelve compounds, docking studies focused on nine hits that exhibited good binding affinities whereas the more negative value indicates stronger binding and comfortable docking conformation [22]. Data for the binding affinity, and the interacting amino acid residues are found in Table 1. From the results of molecular docking studies of chromene derivatives, all the compounds showed good binding interactions with cancer target Rab23 in range of -7.5 to -6.2 kcal/mol as summarized in Table 1. Among the compounds tested, 11-amino-12-(2,3-dimethoxyphenyl)-8,9,10,12-tetrahydro-7H-chromeno[2,3-b]quinolin-3-ol 5c and 11-amino-12-(2,6-dichlorophenyl)-8,9,10,12-tetrahydro-7H-chromeno[2,3-b]quinolin-3-ol 5b were interacted very effectively and showed the least binding scores of -7.9 and -7.5 kcal/mol respectively as represented in Table 1 and Figures 5 and 6.

The chromene derivative **4a** formed hydrogen bond (NH---O) and two π -sigma interactions with

ARG80 at the distance of 2.41, 2.64 and 2.71 Å respectively. Compound **4b** showed H-bond, π -cation and π -sigma interactions with ARG80, LYS22 and ALA19 at the distance of 1.92, 5.69 and 2.63 Å respectively. While, the derivative **1c** exhibited π -cation interaction with ARG80 at the distance of 5.97 Å respectively. The compound **5a** interacted with ARG80 by one hydrogen bond plus two π -cation interactions at 2.19, 5.68 and 5.84 Å respectively. In addition, compound **2b** showed one π - π , three π -cation along with one π -sigma interactions with ARG80 with the distances of 5.08, 3.42, 5.30, 5.97 and 2.79 Å. The compound **5c** exhibited H-bond with ARG80 (NH---O) and THR65 (O---HO) at 1.73 and 1.90 Å, π -cation interaction with LYS22 at 4.83 Å, and π -sigma interaction with ARG80 at 2.70 Å. Compounds **6a** exhibited H-bond and π -cation interactions with ARG80 and LYS11 at the distance of 2.02 and 5.31 Å. Finally, compounds **6b-c** showed π -cation interactions with ARG80 at 5.77, 4.19 and 5.96 Å, as shown in Table 1 and Figures 5. To further understand the nature of docking, arginine ARG contains positively charged guanidinium group $H_2N-C(=NH)-NH-$ that is involved in forming π -cation interaction with electron-rich aromatic systems like phenol, pyridine and pyran moieties of compounds **5a**, **5b**, **6b** and **6c** as declared in Figures 5 and 6. Additionally, lysine LYS contains a positively charged amino on its side-chain that is involved in forming π -cation interaction with compounds **4b**, **5c** and **6a**. On the other hand, tryptophan TRP contains a side chain indole that involved in forming π - π stacking with phenol moiety of compound **5b**. Because of indole is an electron-rich and has H-bond donor (NH), it can participate in various supramolecular interactions with compound **5b**. This clearly demonstrates that indole is a unique chemical moiety in proteins [23]. Interestingly, all the nine compounds bind to the same binding site of Rab23, which is strongly suggested that they have similar mechanism against the cancer target protein. The results show that the compounds tended to have H-bonding, π - π stacking, π -cation, π -sigma interactions. These attractive non-covalent interactions that formed between compounds and Rab23 play a significant role in stabilizing the synthetic compounds at the binding site region [24]. The synthesized molecules with hetero rings (pyran and pyridine) moieties, are observed to be common pharmacophore groups which interact with the functional residues of the cancer target protein through various interactions

as represented in Table 1. The results clearly demonstrated that the newly synthetic compounds are likely to be promising Rab23 protein inhibitor candidates after further refinement.

ADMET profile

In silico absorption, distribution, metabolic, excretion (ADME) and toxicity (T) of the newly synthesized chromene compounds were identified using admetSAR tool, as presented in Table 2. Interestingly all the newly synthesized compounds have a molecular weight in the range of 324-450 (<500). BBB⁺ value describes the ability of the compounds to cross the blood brain barrier, which is in the permissible ranges for all compounds. So they can cross the blood-brain barrier more easily. Also, the values show that the compounds can be absorbed by the human intestines and non-carcinogenic.

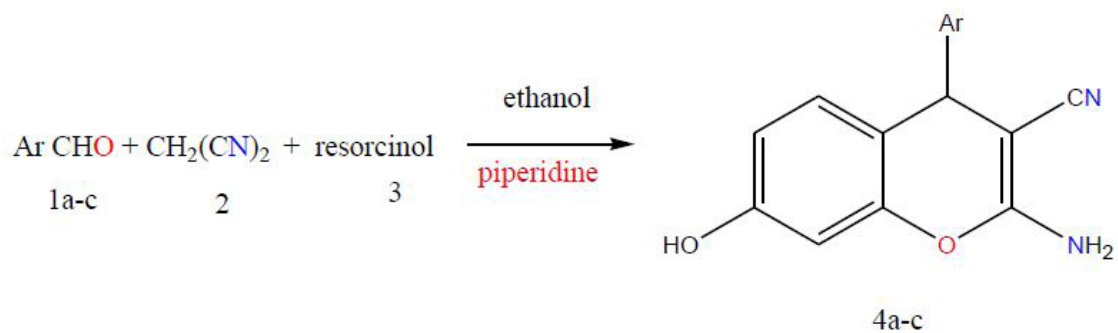
Moreover, the molecules were analyzed for the toxicological potential by the Ames test, using Toxtree tool [25]. The results show that these compounds show better inhibition properties against Rab23 protein, and promising pharmacokinetic properties. Drug-likeness parameters of compounds were calculated using Mol inspiration software, as tabulated in Table 3. The results show interesting values for the compounds as obey Lipinski rule, whereas all the synthesized compounds have molecular weights in the range of 324-450 g/mol (≤ 500), the partition coefficients of the compounds are less than 5. Also, the topological surface areas were found to be in the acceptable range. In addition, the numbers of H-bond acceptors and donors in the tested compounds are in acceptable range. Finally, the synthesized compounds possess high numbers of rotatable bonds (1-4). From all these results, we can conclude that all molecules exhibited good absorption and distribution within the body [26-28]. These ligand molecules may be considered as potent antagonists against Rab23 and used as anti-gastric carcinoma.

Conclusion

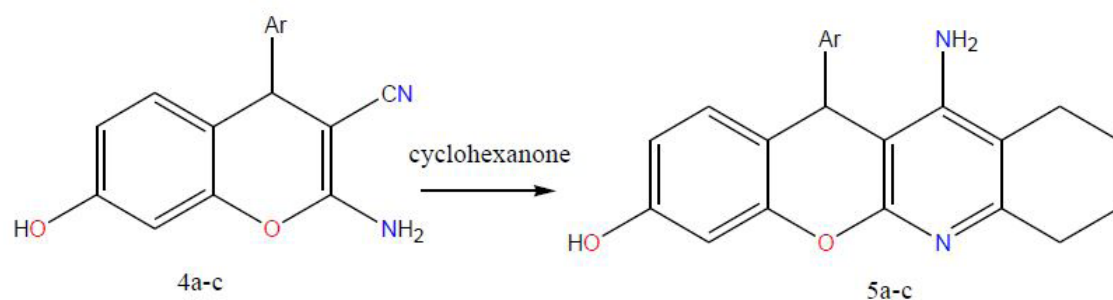
Our study sought to synthesis and identify the new chromene compounds as novel structure leads that could be used in designing Rab23 inhibitor candidates, through computational studies.

References

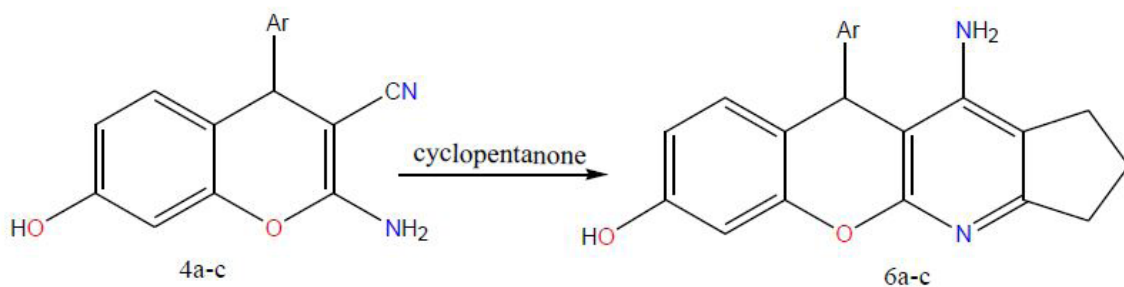
1. Chen Y, Ng F. Rab23 activities and human cancer — emerging connections and mechanisms *Egypt. J. Chem.* Vol. 63, No. 4 (2020)



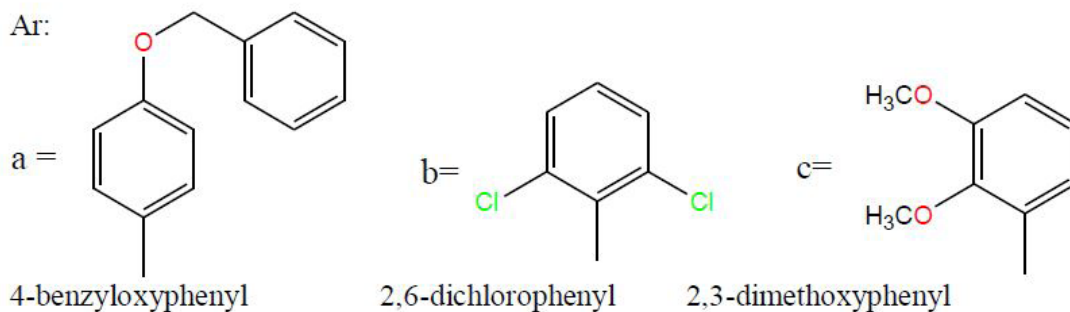
(Scheme 1) Synthesis of 4H-Chromene (4a-c)



Scheme 2 Synthesis of tacrine analogues(5a-c)



Scheme 3. Synthesis of chromenopyridine derivatives(6a-c)



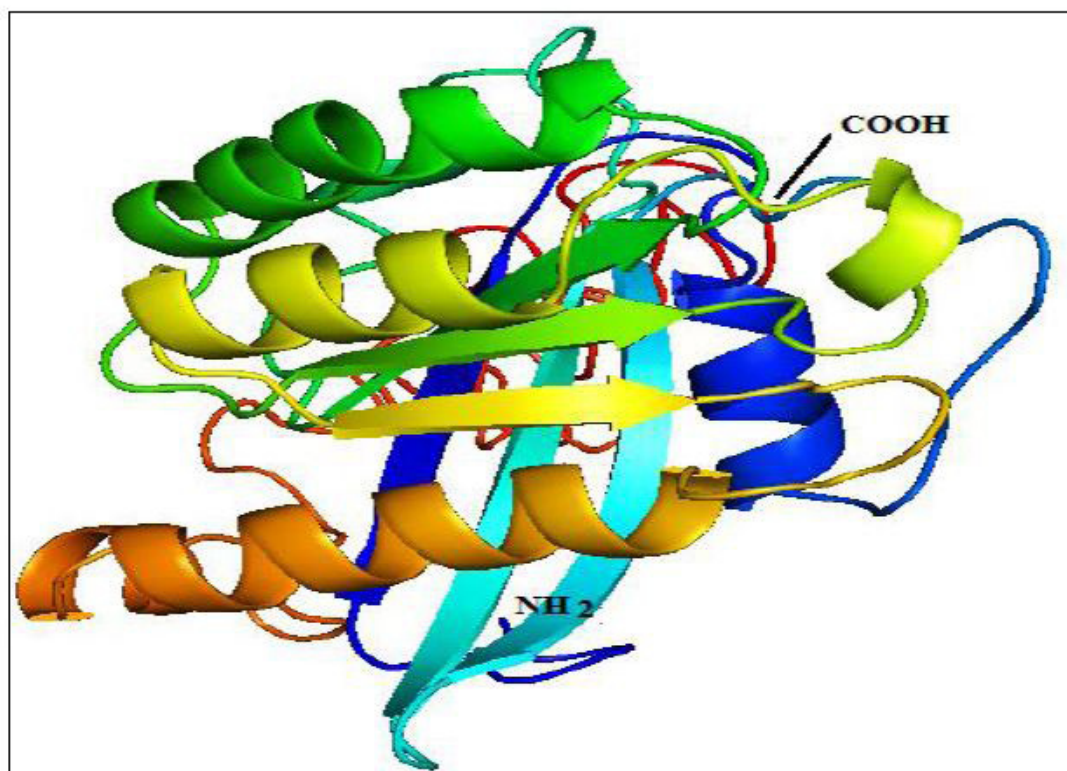


Fig. 1. Three-dimensional structure of Rab23 protein. The 3D model has 9 α - helices and 6 β - sheets, obtained from Modeller 9.11. N-terminal indicates the starting residue and C-terminal indicates the end residue.

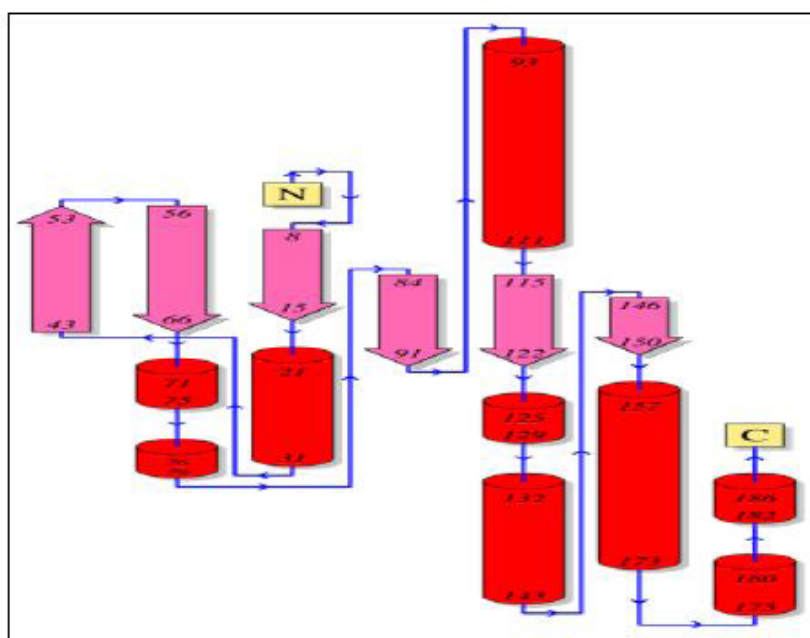


Fig. 2. Schematic diagram of the topological secondary structure of Rab23. The α -helices are shown in red cylinders, while β -strands as pink arrows.

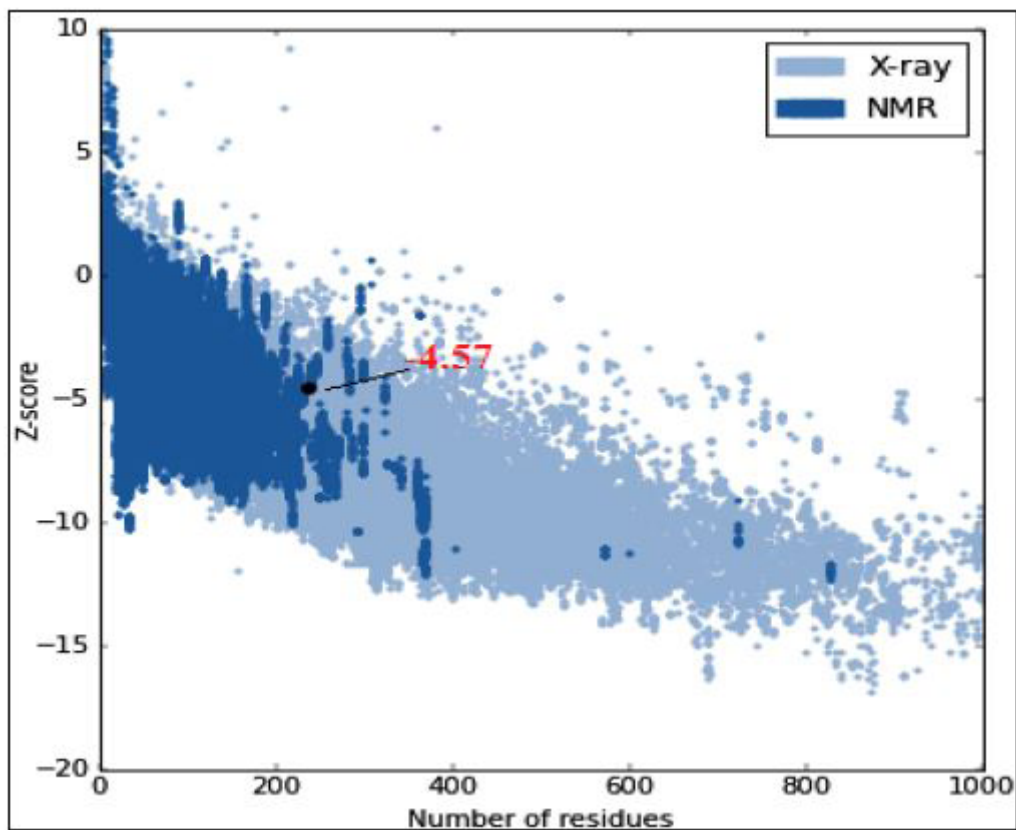


Fig. 3. The local model quality of Rab23. The Z-score of protein (-4.75) falls in the range of PDB proteins submitted by NMR (dark blue region) and X-ray crystallography (light blue region), indicating a good quality model.

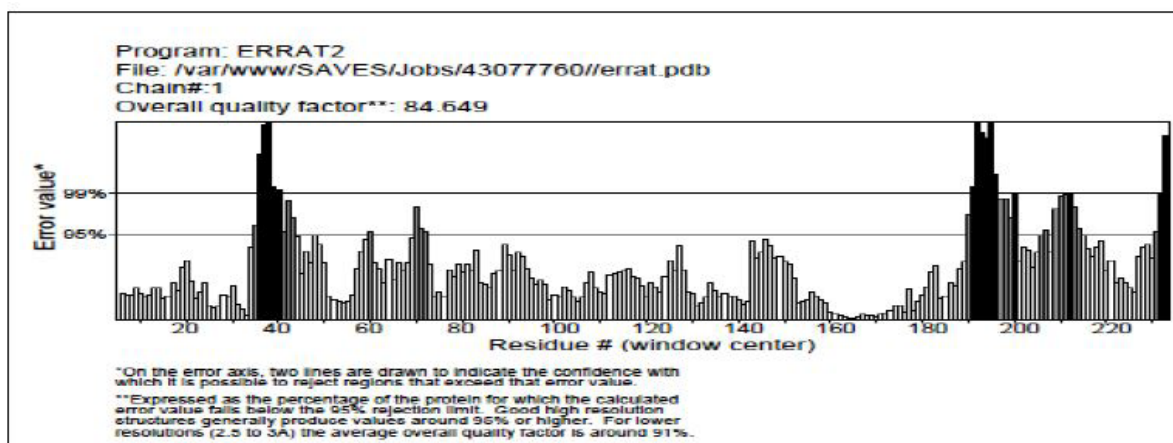
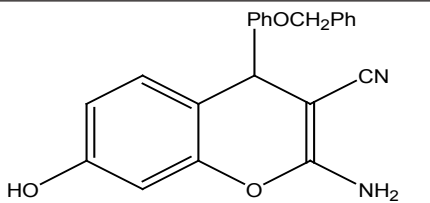
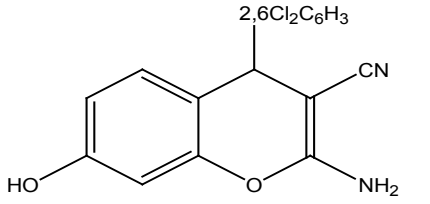
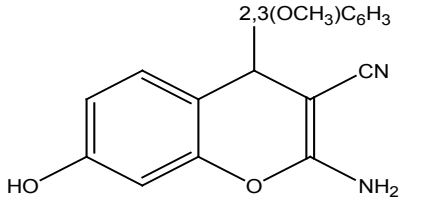
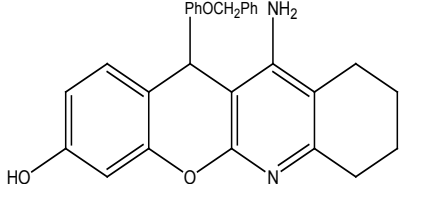
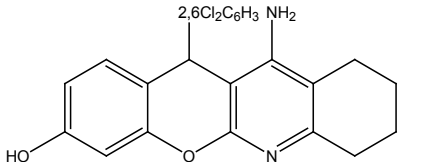
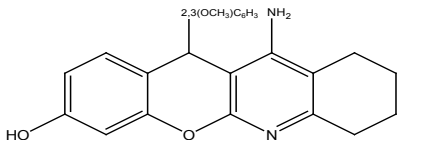
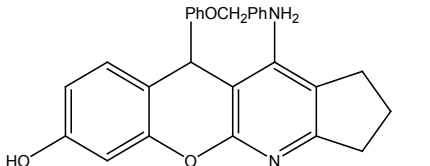
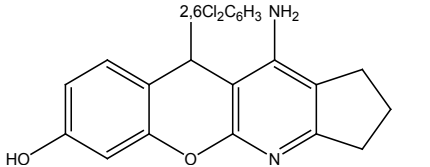
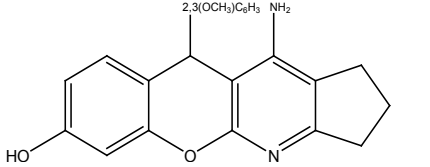


Fig. 4. The overall quality value of Rab23 using ERRAT program. The Errat evaluation method gave 84.64 % as the overall quality factor which is considered to be good enough to use this model. In the Errat, the incorrect regions are shown in black, and the correct regions are shown in gray.

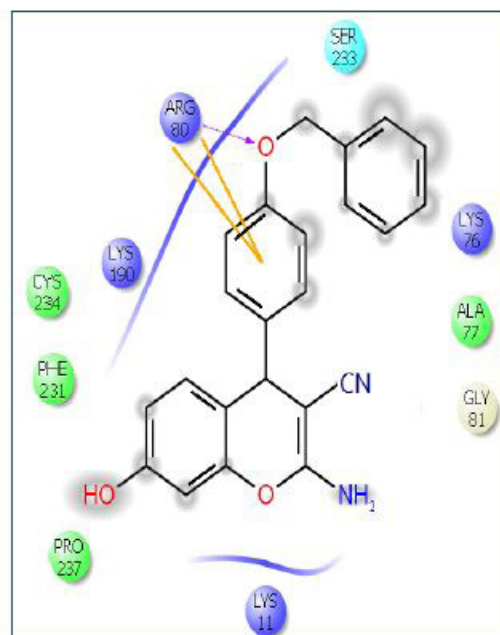
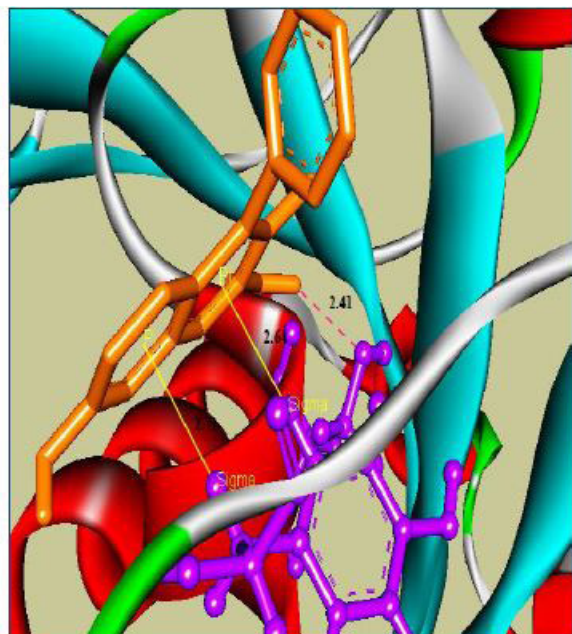
TABLE 1. The binding affinity (kcal/mol) of chromene compounds with Rab23 after molecular docking. The nine molecules (4-6) with the best binding affinity are represented with docking interactions in table, showing H-bonding, π - π , π -cation, and π -sigma interactions.

Structure/Name	Binding affinity (kcal/mol)	Docked complex (amino acid –ligand) interactions	Distance (Å°)
4a  2-Amino-4-(4-benzyloxy-phenyl)-7-hydroxy-4H-chromene-3-carbonitrile	-6.2	H-bonds compound 4a---ARG80 π-sigma interactions compound 4a---ARG80 compound 4a---ARG80	2.41 2.64 2.71
4b  2-Amino-4-(2,6-dichloro-phenyl)-7-hydroxy-4H-chromene-3-carbonitrile	-7.1	H-bonds compound 4b---ARG80 π-cation interactions compound 4b---LYS22 π-sigma interactions compound 4b---ALA19	1.92 5.69 2.63
4c  2-Amino-4-(2,3-dimethoxy-phenyl)-7-hydroxy-4H-chromene-3-carbonitrile	-6.8	π-cation interactions compound 4c---ARG80	5.97
5a  11-Amino-12-(4-(benzyloxy)phenyl)-8,9,10,12-tetrahydro-7H-chromeno[2,3-b]quinolin-3-ol	-6.7	H-bonds compound 5a---ARG80 π-cation interactions compound 5a---ARG80 compound 5a---ARG80	2.19 5.68 5.84

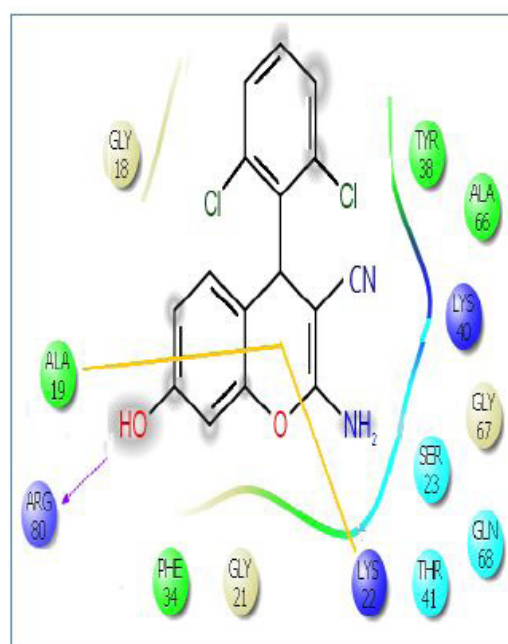
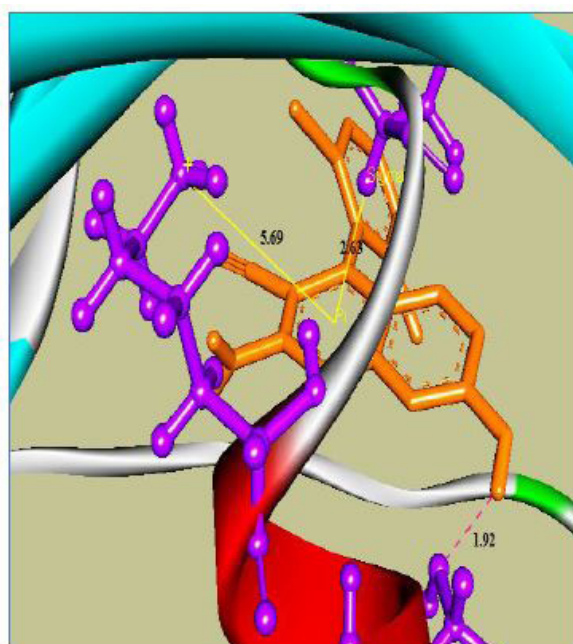
Contd.

5b	 <p>11-amino-12-(2,6-dichlorophenyl)-8,9,10,12-tetrahydro-7H-chromeno[2,3-b]quinolin-3-ol</p>	-7.5	<p>π-π interactions</p> <p>compound 5b---TRP63 5.08</p> <p>π-cation interactions</p> <p>compound 5b---ARG80 3.42</p> <p>compound 5b---ARG80 5.30</p> <p>compound 5b---ARG80 5.97</p> <p>π-sigma interactions</p> <p>compound 5b---ARG80 2.79</p>
5c	 <p>11-amino-12-(2,3-dimethoxyphenyl)-8,9,10,12-tetrahydro-7H-chromeno[2,3-b]quinolin-3-ol</p>	-7.9	<p>H-bonds</p> <p>compound 5c---ARG80 1.73</p> <p>compound 5c---THR65 1.90</p> <p>π-cation interactions</p> <p>compound 5c---LYS22 4.83</p> <p>π-sigma interactions</p> <p>compound 5c---ARG80 2.70</p>
6a	 <p>11-amino-10-(4-(benzyloxy)phenyl)-1,2,3,10-tetrahydrochromeno[2,3-b]cyclopenta[e]pyridin-7-ol</p>	-6.5	<p>H-bonds</p> <p>compound 6a---ARG80 2.02</p> <p>π-cation interactions</p> <p>compound 6a---LYS11 5.31</p>
6b	 <p>11-amino-10-(2,6-dichlorophenyl)-1,2,3,10-tetrahydrochromeno[2,3-b]cyclopenta[e]pyridin-7-ol</p>	-7.0	<p>π-cation interactions</p> <p>compound 6b---ARG80 5.77</p>
6c	 <p>11-amino-10-(2,3-dimethoxyphenyl)-1,2,3,10-tetrahydrochromeno[2,3-b]cyclopenta[e]pyridin-7-ol</p>	-6.1	<p>π-cation interactions</p> <p>compound 6c---ARG80 4.19</p> <p>compound 6c---ARG80 5.96</p>

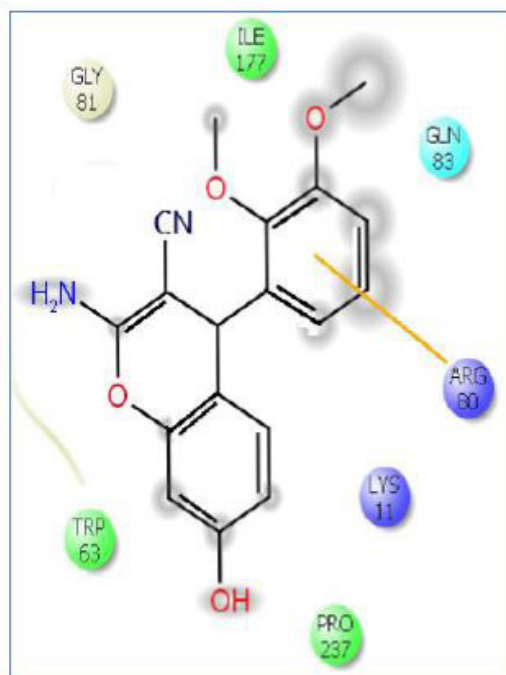
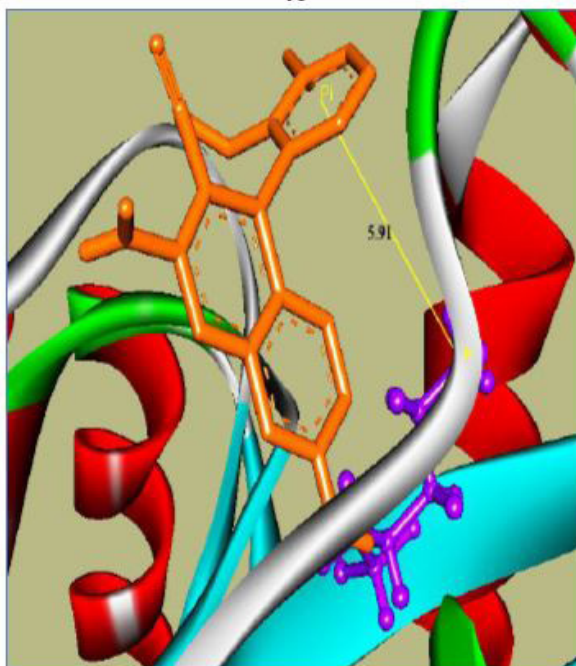
4a



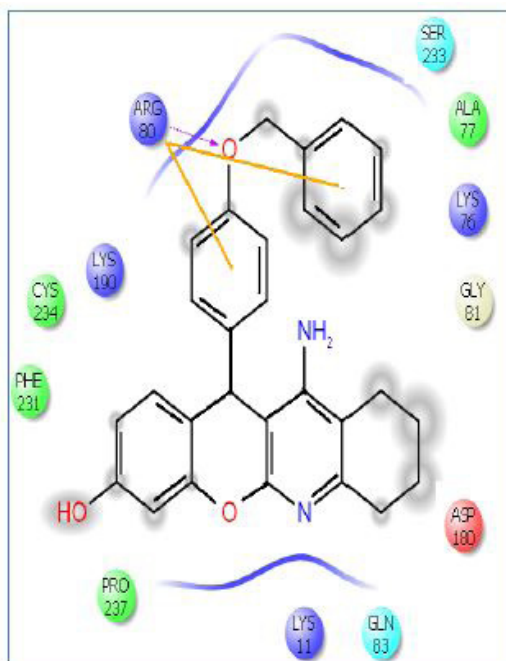
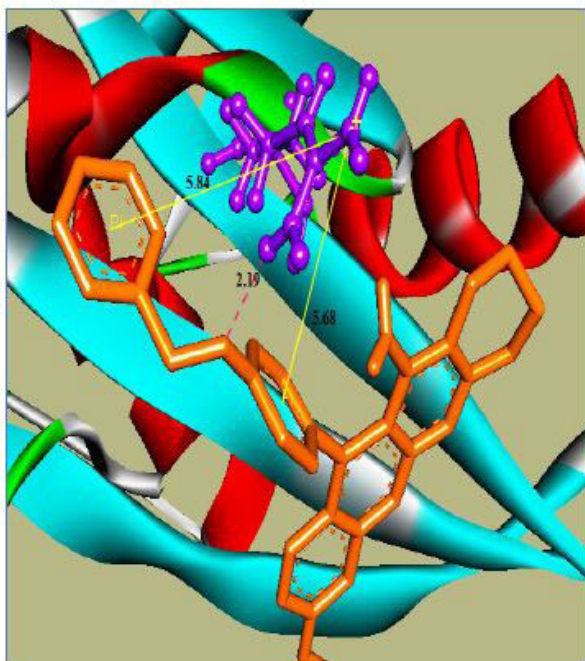
4b



4c

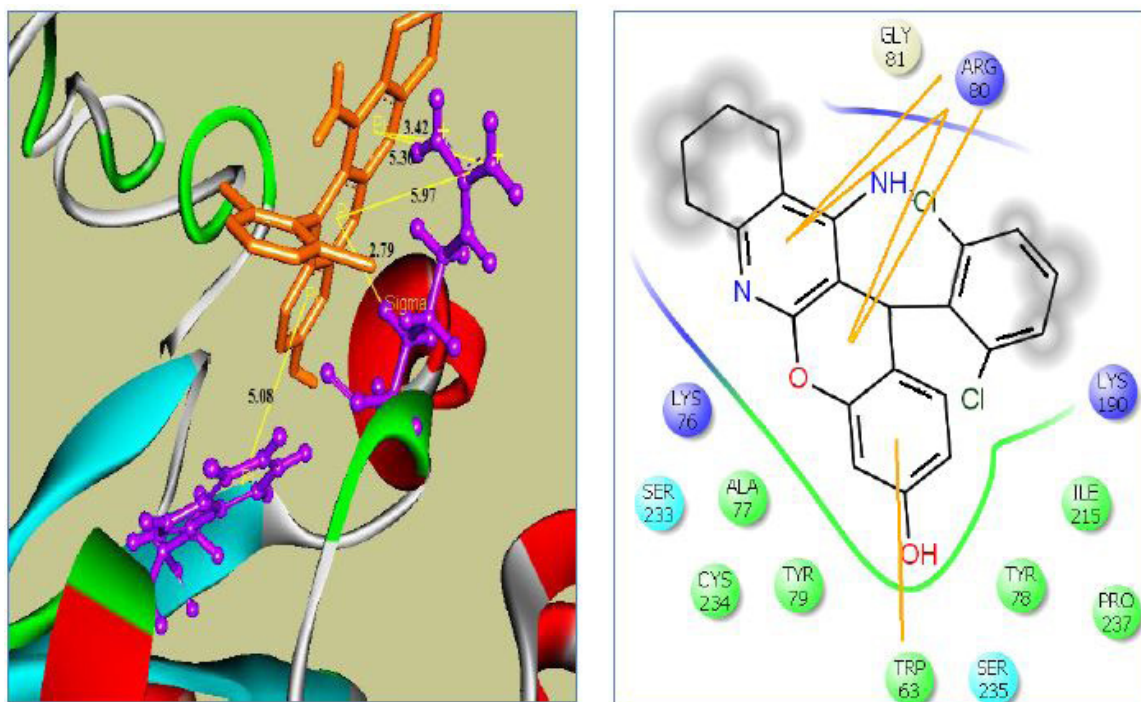


5a

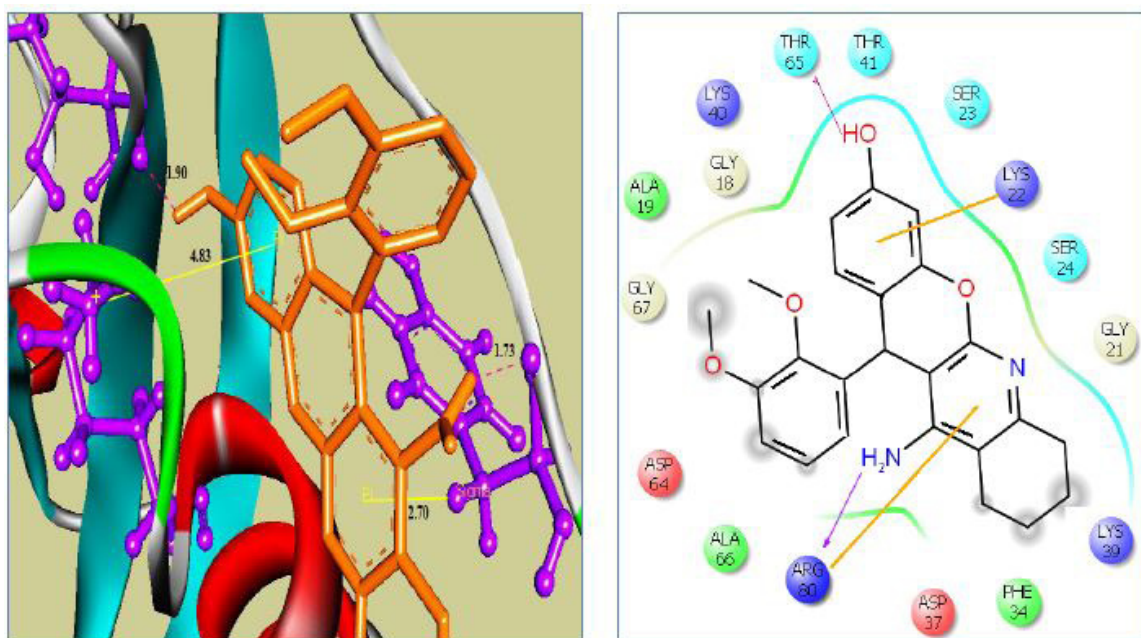


Contd.

5b

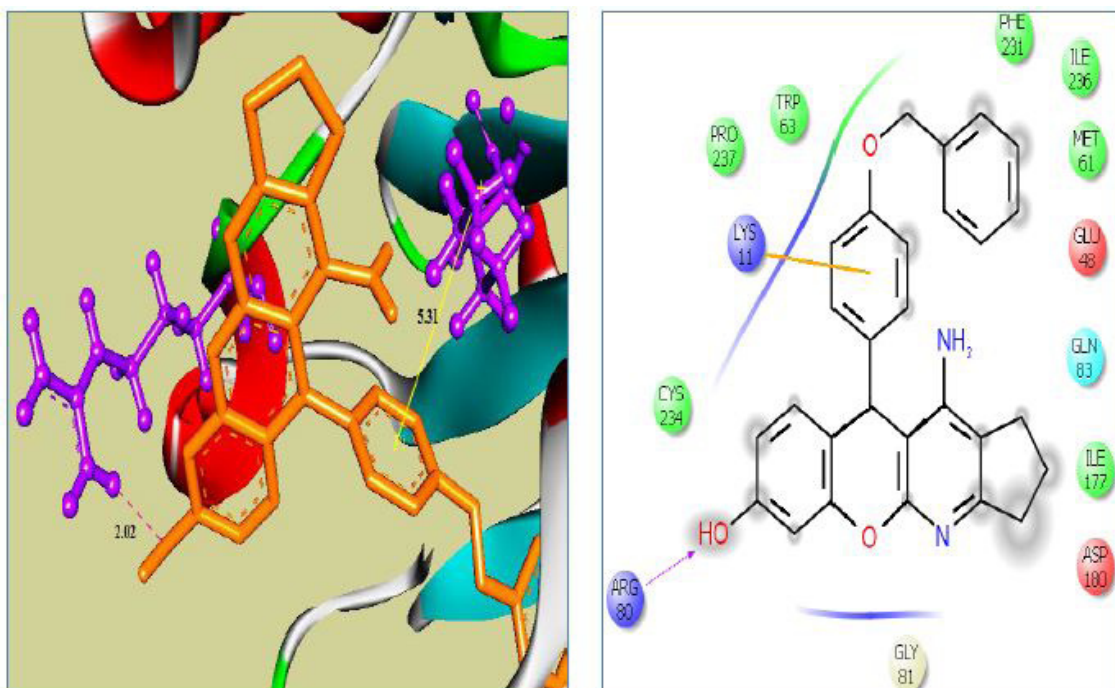


5c

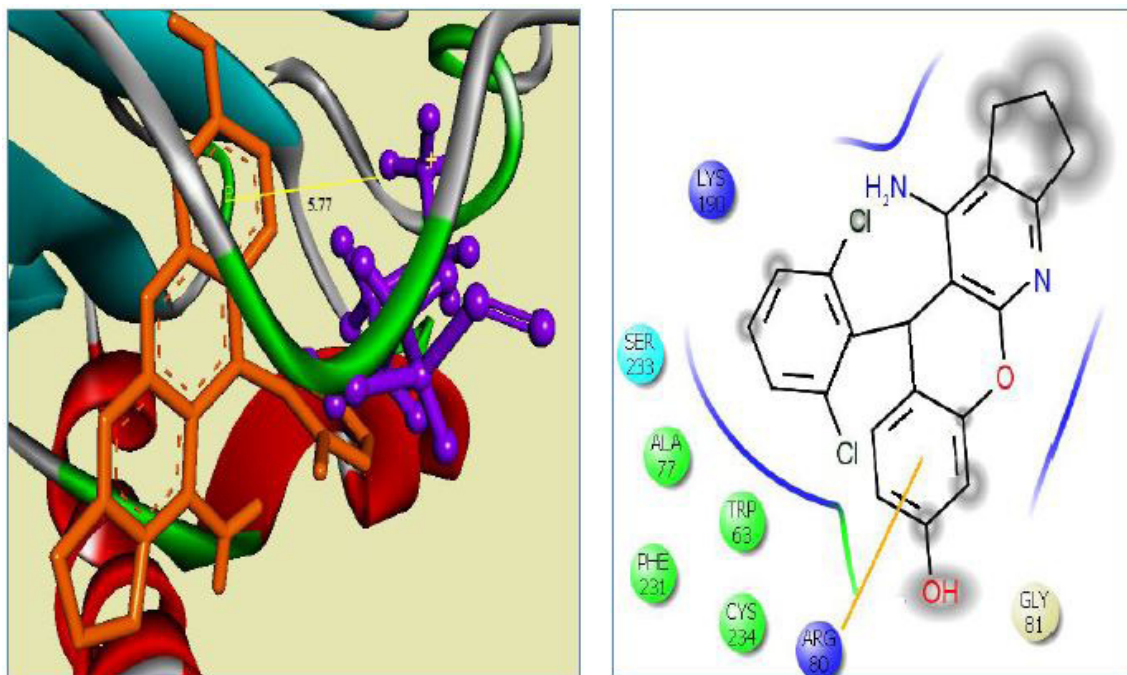


Contd.

6a



6b



Contd.

6c

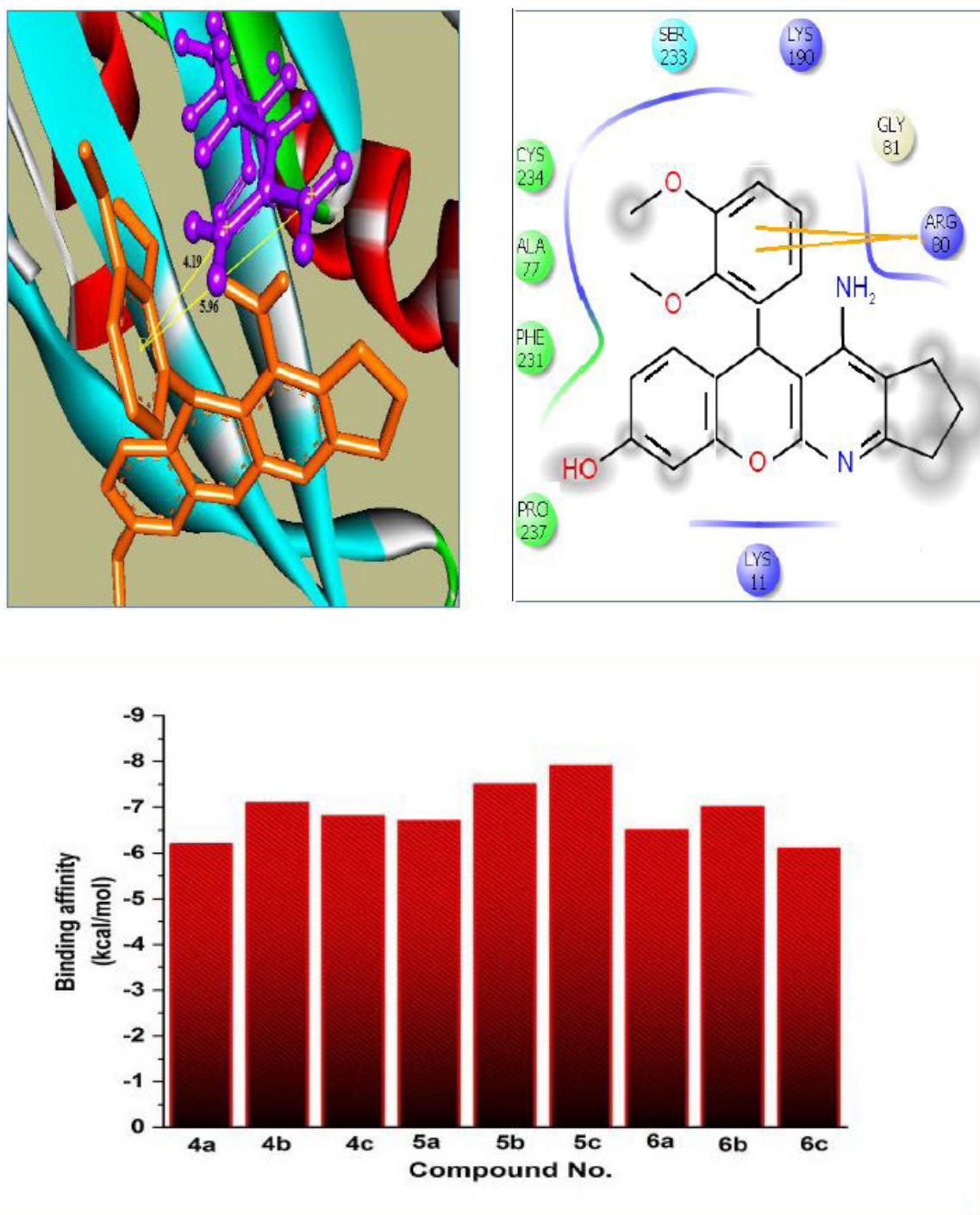


Fig. 6. Relationship between Binding affinity and compound numbers. This chart shows the relationship between binding affinity and compound numbers. The compounds 5c and 5b showed the least binding scores of -7.9 and -7.5 kcal/mol respectively.

TABLE 2. List of ADMET properties of newly synthetic chemical compounds. The pharmacokinetic properties of the molecules (4-6) which form docked complexes with Rab23 protein are evaluated by admetSAR and Toxtree tools.

	Molecular Weight (g/mol)	Blood-Brain Barrier (BBB+)	Human Intestinal Absorption (HIA+)	Caco-2 Permeability (Caco2+)	AMES toxicity	Carcinogenicity
4a	370	0.55	0.98	0.55	Nontoxic	Non carcinogenic
4b	333	0.54	0.99	0.51	Nontoxic	Non carcinogenic
4c	324	0.92	0.94	0.52	Nontoxic	Non carcinogenic
5a	450	0.93	0.98	0.65	Nontoxic	Non carcinogenic
5b	413	0.88	0.99	0.56	Nontoxic	Non carcinogenic
5c	403	0.58	0.92	0.51	Nontoxic	Non carcinogenic
6a	436	0.95	0.98	0.67	Nontoxic	Non carcinogenic
6b	399	0.92	0.99	0.58	Nontoxic	Non carcinogenic
6c	389	0.65	0.94	0.53	Nontoxic	Non carcinogenic

TABLE 3. Physicochemical properties of the title compounds (4-6). logp, logarithm of partition coefficient between n-octanol and water; TPSA, topological polar surface area; HBA, number of hydrogen bond acceptors; HBD, number of hydrogen bond donors; n rotatable, number of rotatable bonds.

	logp	TPSA A ²	HBA	HBD	N violations	N rotatable	Volume A ³
4a	3.89	88.51	5	3	0	4	331.20
4b	3.50	79.28	4	3	0	1	261.08
4c	2.06	97.75	6	3	0	3	285.10
5a	4.98	77.61	5	3	0	4	410.54
5b	4.97	68.38	4	3	0	1	340.42
5c	4.88	73.95	5	3	0	3	368.60
6a	4.78	77.61	5	3	0	4	393.74
6b	4.80	68.38	4	3	0	1	323.62
6c	4.11	73.95	5	3	0	3	351.79

- Introduction — Rabs and human cancer 2018:1–37.
2. Formulation A. Academic Sciences 2013;6:2011–4.
 3. Hafez H. Microwave-Assisted Synthesis and Cytotoxicity Evaluation of Some Novel Pyrazole Containing Imidiazole, Pyrazole, Oxazole, Thiadiazole and Benzochromene derivatives. *Egypt J Chem* 2017;60:5–9. doi:10.21608/ejchem.2017.1824.1151.
 4. Sangani C, Shah N, Patel M, Patel R. Microwave assisted synthesis of novel 4h-chromene derivatives bearing phenoxy pyrazole and their antimicrobial activity assess. *J Serbian Chem Soc* 2012;77:1165–74. doi:10.2298/jsc120102030s.
 5. Patil SA, Wang J, Li XS, Chen J, Jones TS, Hosni-Ahmed A, et al. New substituted 4H-chromenes as anticancer agents. *Bioorganic Med Chem Lett* 2012;22:4458–61. doi:10.1016/j.bmcl.2012.04.074.
 6. El-Maghraby AM. Green Chemistry: New Synthesis of Substituted Chromenes and Benzochromenes via Three-Component Reaction Utilizing Rochelle Salt as Novel Green Catalyst. *Org Chem Int* 2014;2014:1–6. doi:10.1155/2014/715091.
 7. Dallakyan S, Olson A.J. Small-Molecule Library Screening by Docking with PyRx. *Chem. Biol.*, vol. 1263, Springer; 2015, p. 243–50. doi:10.1016/B978-0-12-394447-4.10004-5.
 8. Šali A. Comparative protein modeling by satisfaction of spatial restraints. *Mol Med Today* 1995;1:270–7. doi:10.1016/S1357-4310(95)91170-7.
 9. Wiederstein M, Sippl MJ. ProSA-web: Interactive web service for the recognition of errors in three-dimensional structures of proteins. *Nucleic Acids Res* 2007;35:407–10. doi:10.1093/nar/gkm290.
 10. Colovos C, Yeates TO. Verification of protein structures: Patterns of nonbonded atomic interactions. *Protein Sci* 1993;2:1511–9. doi:10.1002/pro.5560020916.
 11. Huang B. MetaPocket: A Meta Approach to Improve Protein Ligand Binding Site Prediction. *Omi A J Integr Biol* 2009;13:325–30. doi:10.1089/omi.2009.0045.
 12. Konc J, Janežič D. ProBiS: A web server for detection of structurally similar protein binding sites. *Nucleic Acids Res* 2010;38:436–40. doi:10.1093/nar/gkq479.
 13. Cheng F, Li W, Zhou Y, Shen J, Wu Z, Liu G, et al. AdmetSAR: A comprehensive source and free tool for assessment of chemical ADMET properties. *J Chem Inf Model* 2012;52:3099–105. doi:10.1021/ci300367a.
 14. Gasteiger E, Hoogland C, Gattiker A, Duvaud S, Wilkins MR, Appel RD, et al. Protein Identification and Analysis Tools on the ExPASy Server. 2005. doi:10.1385/1-59259-890-0:571.
 15. Altschul SF, Madden TL, Schäffer AA, Zhang J, Zhang Z, Miller W, et al. TLP-1997.pdf 1997;25:3389–402. doi:10.1093/nar/25.17.3389.
 16. Laskowski RA. PDBsum: summaries and analyses of PDB structures. *Nucleic Acids Res* 2002;29:221–2. doi:10.1093/nar/29.1.221.
 17. Krivák R, Hoksza D. Improving protein-ligand binding site prediction accuracy by classification of inner pocket points using local features. *J Cheminform* 2015;7:1–13. doi:10.1186/s13321-015-0059-5.
 18. Soliman A, Kamel M, Eweas A, Wietrzyk J, Milczarek M. The Antiproliferative Activity and Molecular Docking studies of some sulfonamides against cancer cell lines compared to normal cells. *Egypt J Chem* 2018;61:330–40. doi:10.21608/ejchem.2018.2934.1242.
 19. Abid S, Abdula A, Al Marjani M, Abdulhameed Q. Synthesis, Antimicrobial, Antioxidant and Docking Study of Some Novel 3,5-Disubstituted-4,5-dihydro-1H-pyrazoles Incorporating Imine Moiety. *Egypt J Chem* 2018;0:0–0. doi:10.21608/ejchem.2018.5804.1498.
 20. O'Boyle NM, Banck M, James CA, Morley C, Vandermeersch T, Hutchison GR. Open Babel: An Open chemical toolbox. *J Cheminform* 2011;3:33. doi:10.1186/1758-2946-3-33.
 21. Cui M, Mihaly M, Hong-Xing Z, Meng X-Y. Molecular Docking: A powerful approach for structure-based drug discovery. *Curr Comput Aided Drug Des* 2011;7:146–57. doi:10.2174/157340911795677602.
 22. Du X, Li Y, Xia YL, Ai SM, Liang J, Sang P, et al. Insights into protein–ligand interactions: Mechanisms, models, and methods. *Int J Mol Sci*

- 2016;17:1–34. doi:10.3390/ijms17020144.
23. Naim MJ, Alam O, Alam J, Bano F, Alam P, Shrivastava N. Recent review on indole: A privileged scaffold structure. *Int J Pharm Sci Res* 2016;7:51–62.
 24. Bonds SN. The Hydrogen Bond Underlies Water's Chemical and Biological Properties Ionic Interactions Are Attractions between Oppositely Charged Ions 2014:1–7.
 25. Patlewicz G, Jeliaskova N, Safford RJ, Worth AP, Aleksiev B. An evaluation of the implementation of the Cramer classification scheme in the Toxtree software. *SAR QSAR Environ Res* 2008;19:495–524. doi:10.1080/10629360802083871.
 26. Abdelmonsef AH. Computer-aided identification of lung cancer inhibitors through homology modeling and virtual screening. *Egypt J Med Human Genetic* 2019; 20: 6. <https://doi.org/10.1186/s43042-019-0008-3>
 27. Hussein, M. A., Zyaan, O. H., Abdel Monsef, A. H., Rizk, S. A., Farag, S. M., Khaled, A. S., et al. Synthesis, molecular docking and insecticidal activity evaluation of chromones of date palm pits extract against *Culex Pipiens* (Diptera: Culicidae). *Int J Mosq Res* 2018; 5: 22–32.
 28. Abdelmonsef, A. H., Dulapalli, R., Dasari, T., Padmarao, L. S., Mukkera, T., and Vuruputuri, U. (2016). Identification of novel antagonists for Rab38 protein by homology modeling and virtual screening. *Comb Chem High Throughput Screen* 2016; 19: 875–892. doi: 10.2174/1386207319666161026153237